Localized Role of CRMP1 and CRMP2 in Neurite Outgrowth and Growth Cone Steering

Masakazu Higurashi,[1,2] Masumi Iketani,[1] Kohtaro Takei,[1] Naoya Yamashita,[1] Reina Aoki,[1] Nobutaka Kawahara,[2] Yoshio Goshima[1]

[1] Department of Molecular Pharmacology and Neurobiology, Yokohama City University Graduate School of Medicine, Yokohama 236-0004, Japan

[2] Department of Neurosurgery, Yokohama City University Graduate School of Medicine, Yokohama 236-0004, Japan

ABSTRACT: Collapsin response mediator protein 1 (CRMP1) and CRMP2 have been known as mediators of extracellular guidance cues such as semaphorin 3A and contribute to cytoskeletal reorganization in the axonal pathfinding process. To date, how CRMP1 and CRMP2 focally regulate axonal pathfinding in the growth cone has not been elucidated. To delineate the local functions of these CRMPs, we carried out microscale-chromophore-assisted light inactivation (micro-CALI), which enables investigation of localized molecular functions with highly spatial and temporal resolutions. Inactivation of either CRMP1 or CRMP2 in the neurite shaft led to arrested neurite outgrowth. Micro-CALI of CRMP2 in the central domain of the growth cones consistently arrested neurite outgrowth, whereas micro-CALI of CRMP1 in the same region caused significant lamellipodial retraction, followed by retardation of neurite outgrowth. Focal inactivation of CRMP1 in its half region of the growth cone resulted in the growth cone turning away from the irradiated site. Conversely, focal inactivation of CRMP2 resulted in the growth cone turning toward the irradiated site. These findings suggest different functions for CRMP1 and CRMP2 in growth cone behavior and neurite outgrowth. © 2012 Wiley Periodicals, Inc. Develop Neurobiol 72: 1528–1540, 2012

Keywords: CRMP1; CRMP2; CALI; neurite outgrowth; growth cone steering

INTRODUCTION

Development of neural circuitry requires an appropriate axonal pathfinding process, which consists of elastic advance and flexible steering of the growth cone

located at the distal tip of the growing axon. The growth cone plays a central role in this motility through reorganization of cellular cytoskeletons. A number of studies have demonstrated that coordination of the cytoskeleton, i.e., actin filament (AF) and microtubule (MT), at the leading edge of the growth cone and in filopodia is indispensable to accomplish proper asymmetrical motility across the growth cone in accordance with the gradient of diverse extracellular guidance molecules (Challacombe et al., 1997; Nakamura et al., 2001; Fukata et al., 2002a; Zhou and Cohan, 2004; Lowery and Van Vactor, 2009; Tojima et al., 2011).

Collapsin response mediator protein (CRMP) was originally identified as a cytosolic phosphoprotein that mediated semaphorin 3A (Sema3A) signaling (Goshima et al., 1995). CRMP is now known to consist of five homologue proteins CRMP1–5, all of

which are phosphoproteins and are highly expressed in developing nervous systems (Hamajima et al., 1996; Wang and Strittmatter, 1996; Fukada et al., 2000; Yuasa-Kawada et al., 2003; Uchida et al., 2005; Yamashita et al., 2006, 2007, 2011). CRMP has been shown to be an intracellular molecule directly or indirectly regulating cytoskeletal organization and membrane trafficking (Fukata et al., 2002b; Nishimura et al., 2003; Kawano et al., 2005; Rosslenbroich et al., 2005; Schmidt and Strittmatter, 2007; Hensley et al., 2010), which is orchestrated in response to various kinds of extracellular guidance cues, including semaphorins, Reelin, neurotrophins, myelin-derived axonal growth inhibitors, and lysophosphatidic acid (Goshima et al., 1995; Arimura et al., 2000; Quach et al., 2004; Mimura et al., 2006; Uchida et al., 2005, 2009; Yoshimura et al., 2005, 2006, 2011).

Our previous RNAi knockdown or dominant-negative experiments in cultured sensory neurons revealed that both CRMP1 and CRMP2 mediate Sema3A-induced growth cone collapse through their phosphorylation (Uchida et al., 2005). However, respective role of each CRMP family protein in growth cone behavior have not been addressed. To elucidate the local functions of CRMP1 and CRMP2, we conducted a light-mediated acute protein-ablation method called microscale-chromophore-assisted light inactivation (micro-CALI). This method of acute protein ablation uses laser-light irradiation to direct spatially restricted photogenerated hydroxyl radical damage to target proteins through malachite green isothiocyanate (MG)-conjugated antibodies (Jay, 1988; Liao et al., 1994). Micro-CALI allows preferential and acute inactivation of protein functions with highly spatial and temporal resolutions without affecting other cellular functions. Here, we found that CRMP1 and CRMP2 play different roles in neurite outgrowth and growth cone steering.

MATERIALS AND METHODS

Antibodies

Hamster anti-CRMP1 monoclonal antibody (2C6G) was raised as previously described (Yamashita et al., 2006, 2007). Mouse anti-CRMP2 monoclonal antibody (9F) was raised by injection of a C-terminal region of human CRMP2 (amino acid 486–528) into a Balb/c mouse. Their binding specificity was confirmed by immunocytochemistry and immunoblot analysis using COS7 cells and HEK293T cells transfected with each CRMP-Myc (CRMP1–5) expressing vector [Supporting Information Fig. 1(A,B)]. Each CRMP in chick cells were also detected specifically by these antibodies [Supporting Information Fig. 1(C)]. Other antibodies used were anti-tyrosinated-tubulin (rat monoclonal; Harlan Sera-Lab), anti-β-actin (mouse mono-

clonal; Sigma), Cy3-labeled goat anti-Armenian hamster (Jackson ImmunoResearch), Alexa488 or 594-labeled phalloidin, Alexa488 or 594-labeled goat anti-mouse, and Alexa488-labeled donkey anti-rat (Invitrogen).

Cell Culture

A primary dissociated cell culture of chick dorsal root ganglion (DRG) neurons was prepared basically as previously described (Takei et al., 1999). DRG neurons from embryonic Day 7 (E7) chick embryos were dissociated by trypsinization with 0.25% trypsin (Invitrogen) in phosphate-buffered saline (PBS) for 18 min. The neurons were then cultured with Leibovitz-15 medium (Invitrogen) containing nerve growth factor (Wako), glucose, L-glutamine, gentamicin, and fetal bovine serum (Biowest) on a glass base dish (Iwaki) coated with poly-L-lysine (100 μg/mL, Wako) and laminin (10 μg/mL, Invitrogen). The cultured cells were incubated at 37°C for at least 2 h, by which time most neurons had initiated neurite outgrowth.

Immunocytochemistry

Chick DRG cultures were incubated at 37°C for 3 h. The cells were fixed in warmed 4% paraformaldehyde in culture medium at 37°C for 10 min followed by exposure to room temperature for 10 min. After being rinsed with PBS, the cells were permeabilized with 0.1% Triton X-100 (Sigma) in PBS for 5 min, blocked with 1% normal goat serum (Vector) in 0.1% Triton X-100 for 1 h. In case of CRMP2, the neurons were probed primarily with anti-CRMP2 (1:1000) and anti-tyrosinated-tubulin (1:2000) antibodies overnight at 4°C. They were then probed secondarily with fluorescence-conjugated antibodies (1:1000) or rhodamine-conjugated phalloidin (1:250) for 1 h at room temperature. For CRMP1, the cells were additionally altered in 4% formamide at room temperature for 10 min after paraformaldehyde fixation. After the blocking process, the cells were probed primarily with anti-CRMP1 (1:100) and with anti-β-actin (1:1000) or anti-tyrosinated-tubulin antibodies, then probed secondarily with fluorescence-conjugated antibodies (1:1000). The cells were observed at a water-immersed objective of ×63 (C-apochromat/1.2 W korr) with a laser-scanning microscope (LSM510, Carl Zeiss) equipped with an Axioplan 2 imaging microscope (Carl Zeiss). In all cases, matched control immunostainings were carried out with nonimmune immunoglobulin G (IgG) or without a primary antibody. The quantitative analyses of cellular distribution were measured with the Metamorph software program (Molecular Device).

Immunoblot Analysis

Sample lysate was prepared and homogenized in immunoprecipitation buffer [20 mM Tris–HCl, pH 8.0, 150 mM NaCl, 1 mM EDTA, 10 mM NaF, 1 mM Na$_3$VO$_4$, 1% Nonidet P-40, 50 μM ρ-amidinophenylmethanesulfonyl fluoride, and 10 μg/mL of aprotinin]. The lysates were centrifuged at

1200 rpm for 15 min at 4°C, and the supernatants were normalized for total protein concentrations. Proteins were subjected to sodium dodecyl sulfate-polyacrylamide gel electrophoresis (8% gel) in the Laemmli buffer system. After electrophoretic transfer to polyvinylidene fluoride membranes (Millipore, Immobilon), proteins were blocked with 5% skim milk in Tris-buffered saline for 1 h, and then an immunodetection probe with anti-CRMP1 (1:1000) or anti-CRMP2 (1:1000) antibodies was performed and visualized with the enhanced chemifluorescence immunoblotting kit (GE Healthcare).

Micro-CALI

Anti-CRMP1 and anti-CRMP2 antibodies were labeled with MG (dye/protein molar ratio = 6.8; Invitrogen) as previously described (Jay, 1988). The MG-labeled anti-CRMP1 (0.17 mg/mL) or anti-CRMP2 (0.16 mg/mL) antibodies were loaded into DRG neurons by trituration methods as demonstrated previously (Takei et al., 2000). Confirmation of loaded antibodies in living DRG neurons was visualized indirectly by the monitoring of concomitantly loaded fluorescein isothiocyanate (FITC)-conjugated dextran (molecular mass = 150 kDa; Sigma; Takei et al., 2000). MG-labeled nonimmune Armenian hamster IgG (Jackson ImmunoResearch) and MG-labeled nonimmune mouse IgG (Jackson ImmunoResearch), or unlabeled anti-CRMP1 and -CRMP2 antibodies were used for control experiments. The micro-CALI experiment was performed after 2 h incubation after antibody loading. The DRG neuronal culture was maintained at 37°C on a microscope stage incubator throughout the experiment. A neuronal cell selected for complete loading of the MG-labeled antibodies was observed with phase-contrast optics with an ×40 objective lens (Plan Neofluor, Carl Zeiss) for 10 min, and a targeted region (about 15 μm in diameter) of the neuronal cell was subjected to laser irradiation (5 min, wavelength: 620 nm, 20 μJ per pulse at 10 Hz) from a nitrogen-driven dye laser (VSL-337ND and Duo-220, Spectra-Physics), followed by post-CALI 15-min observation. Throughout the 30-min observation, the cell was recorded by time-lapse microscopy (every 5 min) with a cooled charge-coupled device camera (CoolSnap-HQ, Photometrics) and a Windows-based computer equipped with the Metamorph software program. The turning angle of the growth cone was determined by measuring the angle between the growth direction of the distal axon before and after irradiation. The growth direction was shown as a line along the distal axon (20 μm, including the growth cone). The turning angle were quantified every 5 min over a period of 15 min after irradiation.

RESULTS

Distinct Distribution of CRMP1 and CRMP2 in the Growth Cone

To investigate cellular distribution of CRMP1 and CRMP2 in the growth cone, we conducted immuno-

cytochemistry by simultaneously staining actin or tubulin. Although both CRMP1 and CRMP2 were distributed throughout the growth cone, quantitative data showed some differences between them. CRMP1 was uniformly localized throughout the growth cone with subtle tendency of predominance in lamellipodia. CRMP1 in the peripheral domain roughly co-localized with actin [Fig. 1(A)]. Meanwhile, CRMP2 was distributed in the central domain even more than that in the peripheral domain. The quantitative analyses revealed that the proportion of CRMP2 localization was similar to that of tubulin [Fig. 1(B)]. These results indicate that CRMP1 and CRMP2 have distinct distribution in the growth cone.

Inactivation of Either CRMP1 or CRMP2 in the Neurite Shaft Disturbed Neurite Outgrowth

To explore the local function of CRMP1 and CRMP2, we tested the effect of spatial inactivation of endogenous CRMP1 and CRMP2 on neurite outgrowth. We used micro-CALI for molecular targeting in a subregion of the cell where laser light irradiated the neurite shaft. We arbitrarily chose a region that was at least 20 μm distance from both ends of the neurite shaft. Loading of MG-conjugated anti-CRMP1, MG-conjugated anti-CRMP2, or MG-conjugated nonspecific IgG antibodies into DRG neurons by trituration was monitored by the simultaneous loading of FITC-conjugated dextran (Takei et al., 2000). In control micro-CALI experiments, anti-CRMP1 and anti-CRMP2 antibodies without MG labeling were used. The region of interest was irradiated for 5 min, and the growth cone was observed by time-lapse microscopy before, during, and after laser-light irradiation. Inactivation of either CRMP1 or CRMP2 caused temporal growth arrest of neurite outgrowth in a similar way, but no remarkable change in growth cone morphology (Fig. 2). We calculated the rate of growth arrest of the neurites, defined as a greater than 80% reduction of the neurite extension rate for more than 10 min after irradiation. The rate in micro-CALI of CRMP1 was 73% ($n = 15$) but only 19% ($n = 16$) in control experiments (MG-labeled nonspecific IgG). The rate in micro-CALI of CRMP2 was 70% ($n = 10$) but only 20% ($n = 15$) in control experiments. These findings show that in the neurite shaft both CRMP1 and CRMP2 were similarly involved in the molecular events underlying neurite outgrowth.
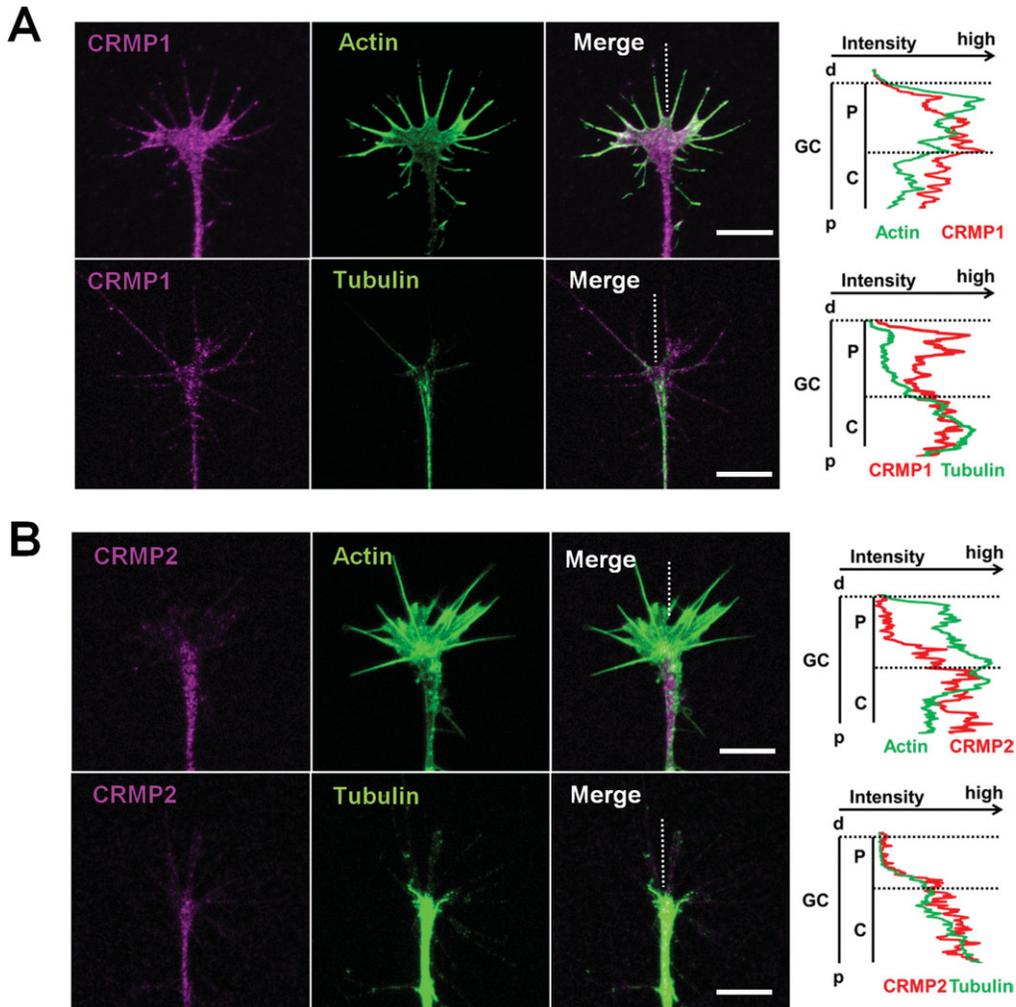
Figure 1 Subcellular localization of CRMP1 (A) and CRMP2 (B) with cytoskeleton components such as actin and tubulin in the growth cone of cultured E7 chick DRG neurons. Quantitative data of their distribution along the sagittal plane at the midline of the growth cone indicated by the dashed white lines in merged pictures are shown in the column on the far right. P; peripheral domain, C; central domain, d; distal, p; proximal, GC; growth cone. Scale bars: 10 μm.

Inactivation of Either CRMP1 or CRMP2 in the Whole Growth Cone Disturbed Neurite Outgrowth in a Different Fashion

To explore whether there are any distinct functions of CRMP1 and CRMP2 in the growth cone compared with those in the neurite shaft, we carried out micro-CALI experiments in the entire region of the growth cone, including the filopodia and lamellipodia. The micro-CALI of either CRMP1 or CRMP2 disturbed neurite extension in the growth cone but a clearly different phenotype was observed for each micro-CALI. Micro-CALI of CRMP1 in the growth cone resulted in a significant reduction of the growth cone area before temporal neurite outgrowth perturbation, and the magnitude of the growth arrest was less than that

in micro-CALI of CRMP1 in the neurite shaft [Fig. 3(A–C)]. Micro-CALI of CRMP2 in the growth cone resulted in arrested outgrowth of neurites without a morphological change in the lamellipodia. This phenotype was similar to that seen in micro-CALI of CRMP2 in the neurite shaft [Fig. 3(A,D,E)]. We calculated the rate of growth arrest of neurites under the above-mentioned definition and the rate of lamellipodial retraction, defined as a greater than 20% reduction of growth cone area for more than 10 min after irradiation. The rate of growth arrest in micro-CALI of CRMP1 was 50% (n = 14) but only 15% (n = 13) in the control experiment. The lamellipodial retraction rate in CRMP1 was 57% (n = 14), whereas no retraction was found in the control experiment

(n = 13) [Fig. 3(A–C)]. The growth arrest rate in micro-CALI of CRMP2 was 87% (n = 30) but only 20% (n = 15) in the control experiment. The lamelli-

podial retraction rate was 21% (n = 28) in CRMP2 but only 10% (n = 10) in the control experiment [Fig. 3(A,D,E)]. These findings suggest that both CRMP1
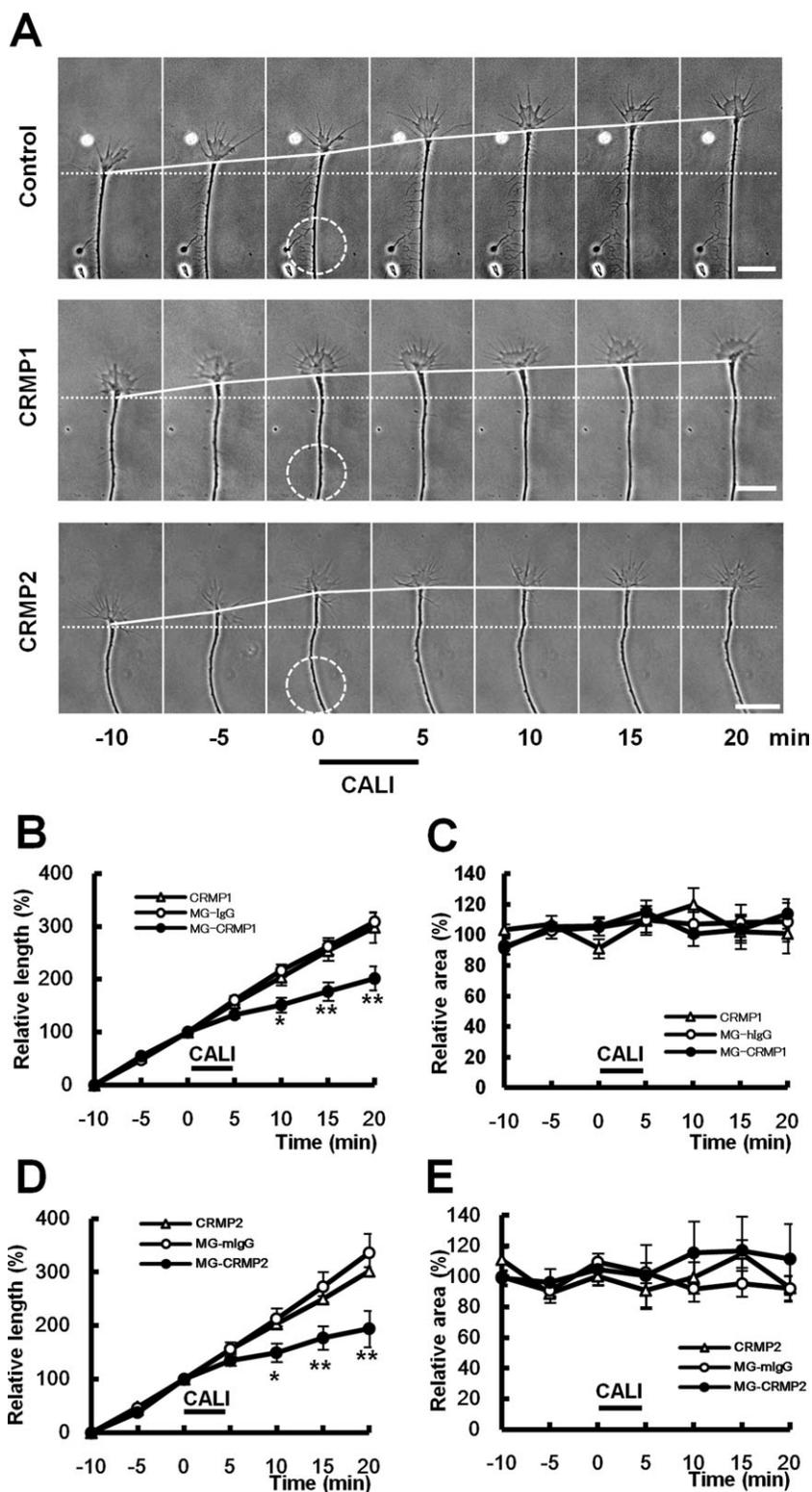

Figure 2

and CRMP2 participated in the molecular events related to neurite outgrowth in the growth cone, but CRMP1 specifically affected growth cone morphology.

Focal Inactivation of Either CRMP1 or CRMP2 in the Growth Cone Induces Growth Cone Turning in Opposite Directions

To scrutinize the function of CRMP1 and CRMP2 in growth cone behavior in more detail, we carried out asymmetrical inactivation of CRMP1 and CRMP2 in the growth cone. Micro-CALI of CRMP1 within a half region of the growth cone resulted in the growth cone turning away from the irradiated side after focal retraction of the irradiated portion of lamellipodia [Fig. 4(A)]. The maximum difference of the turning angle compared with the control micro-CALI experiment was measured at 15 min after irradiation [Fig. 4(C)]. Figure 4(E) displays the cumulative distribution plots of the turning angles at 15 min after laser irradiation. In contrast, micro-CALI of CRMP2 within a half region of the growth cone induced the growth cone to turn toward the irradiated side along the boundary of the laser spot [Fig. 4(B)]. During irradiation, the growth cone never entered the laser spot. Conversely, once the central domain entered the spot entirely, most growth cones exhibited arrested growth or collapse. The difference in the turning angle compared with control-CALI reached the maximum at 10 min after laser irradiation [Fig. 4(D)],

which indicated a more rapid onset of turning compared with micro-CALI of CRMP1. Figure 4(F) depicts the cumulative distribution plots of turning angles at 10 min after laser irradiation. Because this turning occurred without preceding lamellipodial retraction or protrusion, we speculated that this turning was directed by MT protrusion in micro-CALI of CRMP2. Immunocytochemistry of tubulin was carried out by fixing the cell after irradiation before turning onset, and revealed protrusion of MTs along the boundary of the laser spot but little assembly of tubulin in the irradiated area [Fig. 5(A)]. The growth cone after micro-CALI of CRMP2 in the half region of the growth cone was eventually directed to the irradiated side with asymmetric MT assembly. To examine this MT asymmetric distribution quantitatively, we calculated the relative fluorescence intensity of each cytoskeleton, defined as the average intensity in the irradiated half region of the growth cone divided by that in the nonirradiated half region. The relative intensity of tubulin, but not actin, in micro-CALI of CRMP2 was significantly higher than that in control-CALI using MG-IgG antibodies [Fig. 5(B)]. These findings suggest that CRMP1 and CRMP2 play different roles in growth cone steering.

DISCUSSION

Our present findings suggest that both CRMP1 and CRMP2 play important and different roles in neurite outgrowth and growth cone steering. CRMP2 was

Figure 2 Micro-CALI of CRMP1 or CRMP2 in the neurite shaft of cultured E7 chick DRG neurons. (A) The growth cone behavior in micro-CALI of CRMP1, CRMP2 or control micro-CALI using nonspecific IgG. The growth cone is first observed for 10 min before laser irradiation (from −10 to 0 min). The laser is irradiated at the time from 0 to 5 min as indicated by the black line. A dotted circle indicates a laser spot. A solid line indicates the level of the base of the growth cone. A dotted line reveals the original level of the base of the growth cone. Scale bars: 10 μm. (B and D) Quantitative analyses of neurite length in micro-CALI of CRMP1 (nonlabeled anti-CRMP1 antibodies (CRMP1; $n = 11$), MG-labeled nonspecific hamster IgG (MG-hIgG; $n = 16$), and MG-labeled anti-CRMP1 antibodies (MG-CRMP1; $n = 15$) (B)) and in micro-CALI of CRMP2 (nonlabeled anti-CRMP2 antibodies (CRMP2; $n = 10$), MG-labeled nonspecific mouse IgG (MG-mIgG; $n = 15$), and MG-labeled anti-CRMP2 antibodies (MG-CRMP2; $n = 10$) (D)). The laser is irradiated at the time from 0 to 5 min as indicated by the thick black line. The data show mean relative neurite length calculated as 100% of the mean extending neurite length for 10 min before CALI (from −10 to 0 min) and standard error of mean (SEM). *$p < 0.05$, **$p < 0.01$ by one-way ANOVA test. (C and E) Quantitative analyses of growth cone area in micro-CALI of CRMP1 (nonlabeled anti-CRMP1 antibodies (CRMP1; $n = 11$), MG-labeled nonspecific hamster IgG (MG-hIgG; $n = 14$), and MG-labeled anti-CRMP1 antibodies (MG-CRMP1; $n = 15$) (C)) and in micro-CALI of CRMP2 (nonlabeled anti-CRMP2 antibodies (CRMP2; $n = 9$), MG-labeled nonspecific mouse IgG (MG-mIgG; $n = 14$), and MG-labeled anti-CRMP2 antibodies (MG-CRMP2; $n = 10$) (E)). The data depict the mean relative growth cone area calculated as 100% of the means for 10 min before CALI (from −10 to 0 min) and SEM. *$p < 0.05$, **$p < 0.01$ by one-way ANOVA test.

involved in regulation of neurite outgrowth in both the neurite shaft and the growth cone. In contrast, the function of CRMP1 in neurite shafts is associated with neurite outgrowth, whereas that in growth cones is also associated with growth cone morphology. Our present study suggests a cooperative role for CRMP1
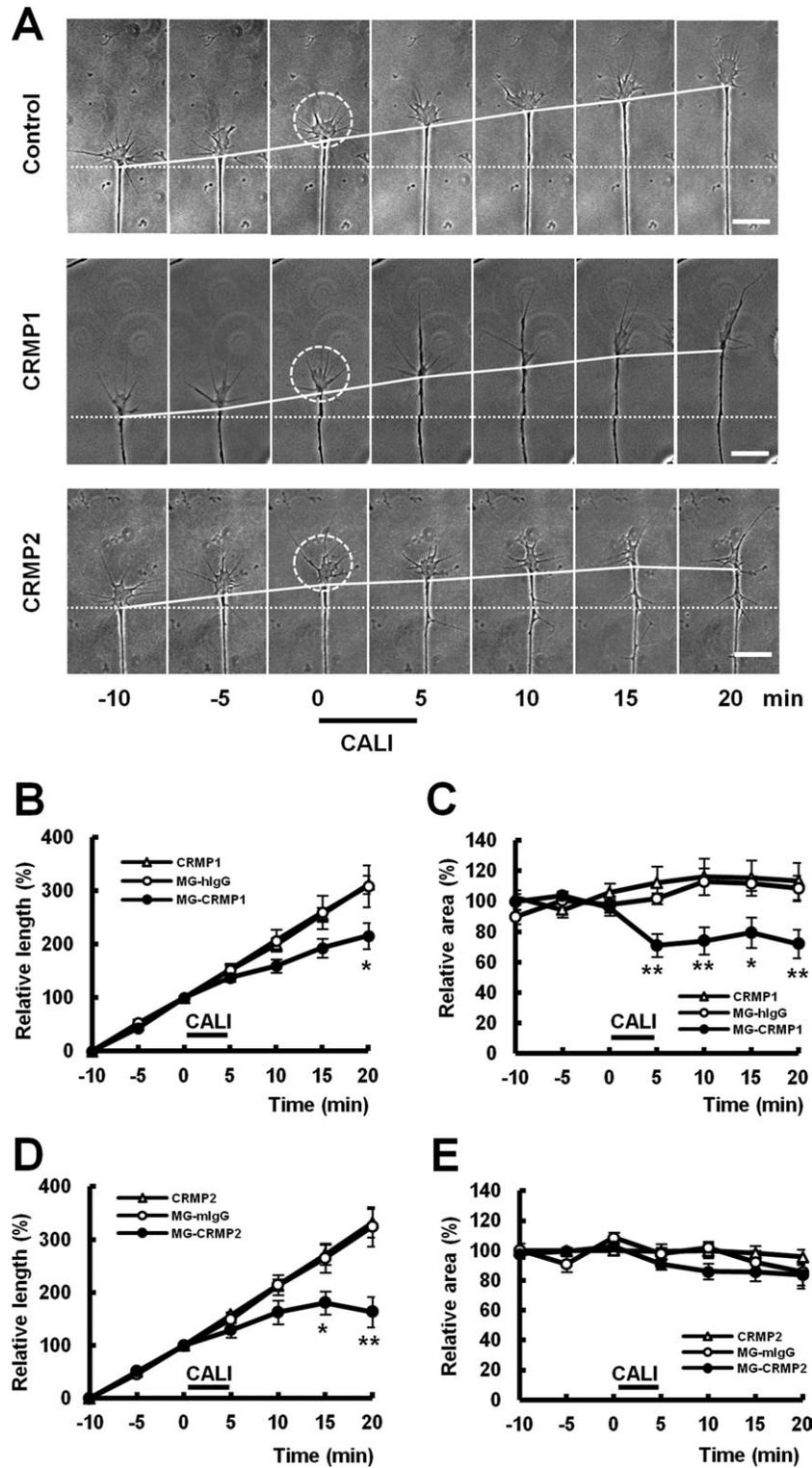

Figure 3

and CRMP2 in the growth cone that contributes to the regulation of neurite outgrowth and growth cone steering. Because both CRMP1 and CRMP2 mediate Sema3A-induced growth cone collapse (Uchida et al., 2005), combination of these different roles may contribute to sophisticated capabilities of growth cones for detecting extracellular guidance cues.

Previous reports performing RNAi and overexpression of dominant-negative forms show that CRMP1 and CRMP2 play a role in facilitating neurite outgrowth by tubulin assembly, membrane trafficking, and actin reorganization (Inagaki et al., 2001; Fukata et al., 2002b; Nishimura et al., 2003; Quach et al., 2004; Kawano et al., 2005). Consistently, our results in micro-CALI of CRMP1 or CRMP2 in the whole growth cone or the axonal shaft demonstrated perturbation of neurite elongation, suggesting that CRMP1 and CRMP2 facilitate neurite outgrowth. Thus, CRMP1 and CRMP2 function could be effectively inactivated by our micro-CALI experiment. Meanwhile, if direct damage to binding cytoskeleton occurred, morphological change would appear more immediately after the start of irradiation. In contrast, in our current study, almost all the phenotypes gradually occurred approximately 5 min after the start of irradiation, as did previous CALI experiments targeting other cytoskeletal binding proteins; filopodial retraction (2–3 min after irradiation) in micro-CALI of myosin-V (Wang et al., 1996), lamellipodial retraction (3–5 min after irradiation) in CALI of MAP1B (Mack et al., 2000). We therefore conclude that micro-CALI of CRMP1 or CRMP2 is not involved in direct inactivation of cytoskeletons.

Among CRMP family members, CRMP2 has been well studied because of its prominent expression during neural development (Wang and Strittmatter, 1996). Previous *in vitro* experiments describe CRMP2 as having an important function in axon specification, elongation, and branching (Inagaki et al., 2001; Fukata et al., 2002b; Nishimura et al., 2003; Kimura et al., 2005; Uchida et al., 2005; Yoshimura et al., 2005; Rahajeng et al., 2010). CRMP2 plays an essential role in transportation of tubulin along MTs via kinesin motor proteins and in assembling tubulin at the plus end of MTs (Fukata et al., 2002b; Kimura et al., 2005; Rahajeng et al., 2010). The arrest of neurite extension by micro-CALI of CRMP2 in the neurite shaft and the growth cone is probably due to the disruption of tubulin assembling in the neurite.

In contrast, the function of CRMP1 is less clear. We formerly reported that CRMP1 is associated with neurite patterning based on the phenotype in *CRMP1-*deficient mice, suggesting that CRMP1 would be involved in neurite extension that is unlikely to be covered by redundant effects of other CRMP family proteins (Charrier et al., 2006; Yamashita et al., 2006, 2007; Su et al., 2007; Buel et al., 2010). However, the function of CRMP1 has been thought to be similar to that of CRMP2 because of the analogous amino acid sequences, conformation, phosphorylation sites, and binding affinity to tubulin (Fukata et al., 2002b; Deo et al., 2004). Furthermore, both CRMP1 and CRMP2 are intracellular mediators of Sema3A signaling, and RNAi of each protein inhibits Sema3A-induced growth cone collapse alike (Uchida et al.,

Figure 3 Micro-CALI of CRMP1 or CRMP2 in the whole growth cone of cultured E7 chick DRG neurons. (A) The growth cone behavior in micro-CALI of CRMP1, CRMP2 or control micro-CALI using nonspecific IgG. The growth cone is first observed for 10 min before laser irradiation (from -10 to 0 min). The laser is irradiated at the time from 0 to 5 min as indicated by the black line. A dotted circle indicates a laser spot. A solid line indicates the level of the base of the growth cone. A dotted line reveals the original level of the base of the growth cone. Scale bars: 10 μm. (B and D) Quantitative analyses of neurite length in micro-CALI of CRMP1 (nonlabeled anti-CRMP1 antibodies (CRMP1; $n = 12$), MG-labeled nonspecific hamster IgG (MG-hIgG; $n = 13$), and MG-labeled anti-CRMP1 antibodies (MG-CRMP1; $n = 14$) (B)), and in micro-CALI of CRMP2 (nonlabeled anti-CRMP2 antibodies (CRMP2; $n = 6$), MG-labeled nonspecific mouse IgG (MG-mIgG; $n = 15$), and MG-labeled anti-CRMP2 antibodies (MG-CRMP2; $n = 30$) (D)). The laser is irradiated at the time from 0 to 5 min as indicated by the thick black line. The data show mean relative neurite length calculated as 100% of the mean extending neurite length for 10 min before CALI (from -10 to 0 min) and standard error of mean (SEM). $*p < 0.05$, $**p < 0.01$ by one-way ANOVA test. (C and E) Quantitative analyses of growth cone area in micro-CALI of CRMP1 (nonlabeled anti-CRMP1 antibodies (CRMP1; $n = 14$), MG-labeled nonspecific hamster IgG (MG-hIgG; $n = 13$), and MG-labeled anti-CRMP1 antibodies (MG-CRMP1; $n = 12$) (C)), and in micro-CALI of CRMP2 (nonlabeled anti-CRMP2 antibodies (CRMP2; $n = 6$), MG-labeled nonspecific mouse IgG (MG-mIgG; $n = 10$), and MG-labeled anti-CRMP2 antibodies (MG-CRMP2; $n = 28$) (E)). The data depict the mean relative growth cone area calculated as 100% of the mean for 10 min before CALI (from -10 to 0 min) and SEM. $*p < 0.05$, $**p < 0.01$ by one-way ANOVA test.
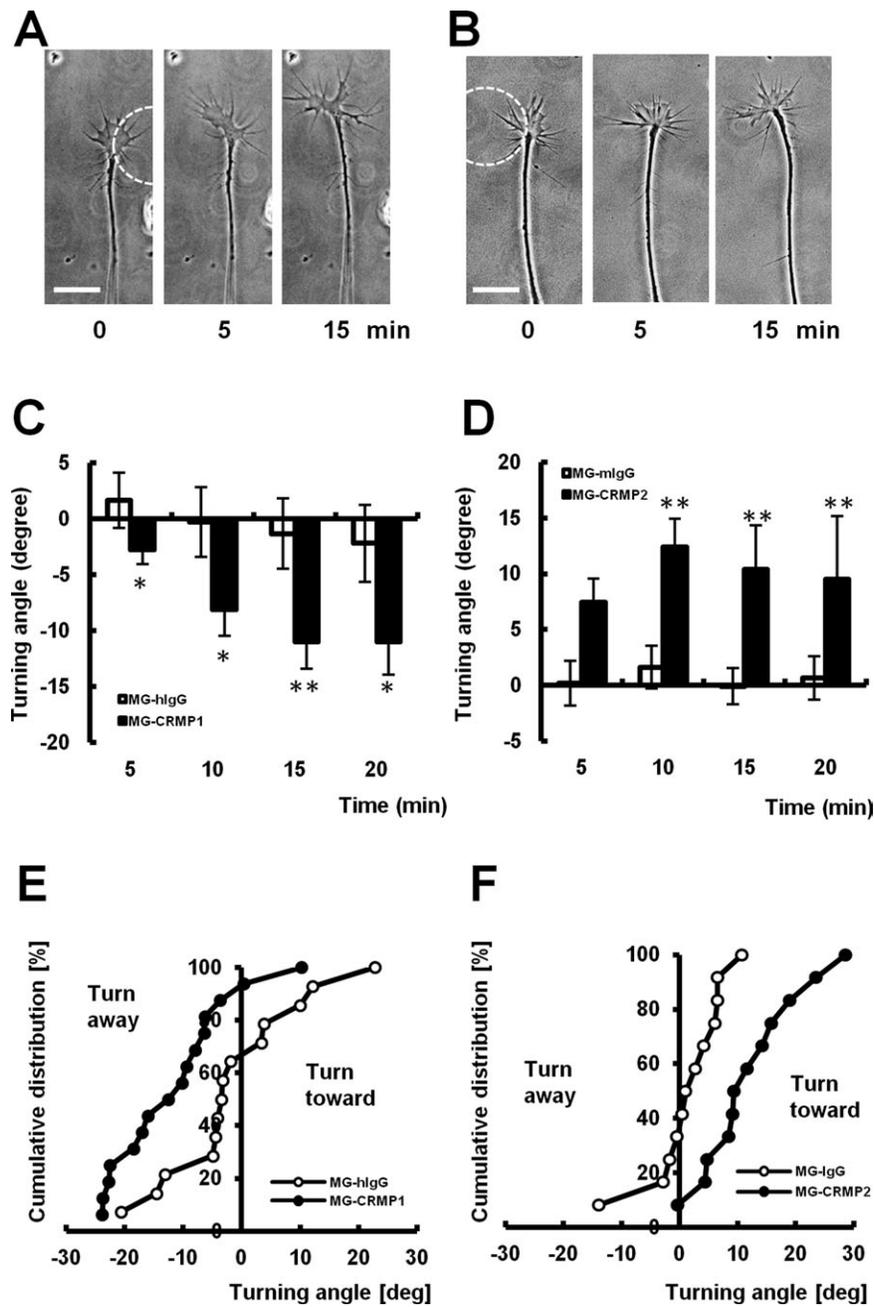
Figure 4 Focal inactivation of CRMP1 or CRMP2 in the growth cone of E7 chick DRG neurons. The growth cone behaviors after focal inactivation of CRMP1 in the right half of the growth cone (A) and CRMP2 in the left half (B) are shown. Time indicates an interval from the start of laser irradiation. A dotted circle describes the laser spot. Scale bars: 10 μm. Turning angles (degree) of the axon growth direction after micro-CALI of CRMP1 (C) and CRMP2 (D) are shown. Time indicates an interval from the start of laser irradiation. *$p < 0.05$, **$p < 0.01$ by Student unpaired *t*-test. Error bars represent SEM. Cumulative distribution plots of turning angles 15 min after the start of irradiation in CRMP1 ($n = 14$) and control ($n = 16$) (E), and 10 min after irradiation in CRMP2 ($n = 12$) and control ($n = 12$) (F) are shown. Positive values for the turning angle depict a change in direction toward the irradiated side and negative values indicate a turning away from the irradiated side.

2005). Therefore, we hypothesized that both CRMPs play similar roles in neurites and growth cones. However, micro-CALI of CRMP1 in the growth cone resulted in a phenotype different from that of micro-CALI of CRMP2. Although CRMP2 inactivation showed a similar phenotype in micro-CALI of CRMP2 in both the neurite shaft and the growth cone, CRMP1 inactivation in the growth cone led to significant lamellipodial retraction and a lesser degree of growth arrest compared with micro-CALI of CRMP1 in the neurite shaft. The different phenotypes in CRMP1- and CRMP2-targeted neurons may be

due to their distinct cellular distribution. Because CRMP2 is well overlapped with tubulin as shown in the previous reports either (Fukata et al., 2002b; Arimura et al., 2005), CRMP2 seems to be mostly devoted to tubulin assembly and less involved in lamellipodial reorganization. In contrast, CRMP1 within the growth cone was localized to the leading edge and appeared to be more associated with actin reorganization. Taken together, these results suggest that CRMP1 and CRMP2 may have different molecular properties associated with cytoskeleton components.

The mechanisms of growth cone turning in response to various kinds of axon guidance molecules have been extensively studied, but the precise mechanisms remain largely unknown (Fan and Raper, 1995; Challacombe et al., 1997; Yuan et al., 2003). Prominent features of the growth cone after focal inactivation of CRMP1 or CRMP2 in its half region are turning-away and turning-toward phenotypes, respectively. Again, this different phenotype might be due to their different functions of CRMP1 and CRMP2 in the regulation of neuronal cytoskeletal proteins. Lamellipodial membrane is supported by mesh of AFs and that the AFs' dynamic properties are essential for lamellipodial protrusion (Lowery and Van Vactor, 2009; Hu and Papoian, 2010). Therefore, the reduction in growth cone area observed in micro-CALI of CRMP1 supports the idea that CRMP1 may contribute to neurite outgrowth mechanism through regulation of actin reorganization. Actin plays an important role not only in lamellipodial formation but also in generation of the cell's advancing force. A growing evidence suggests that the driving force is generated by F-actin retrograde flow and interaction
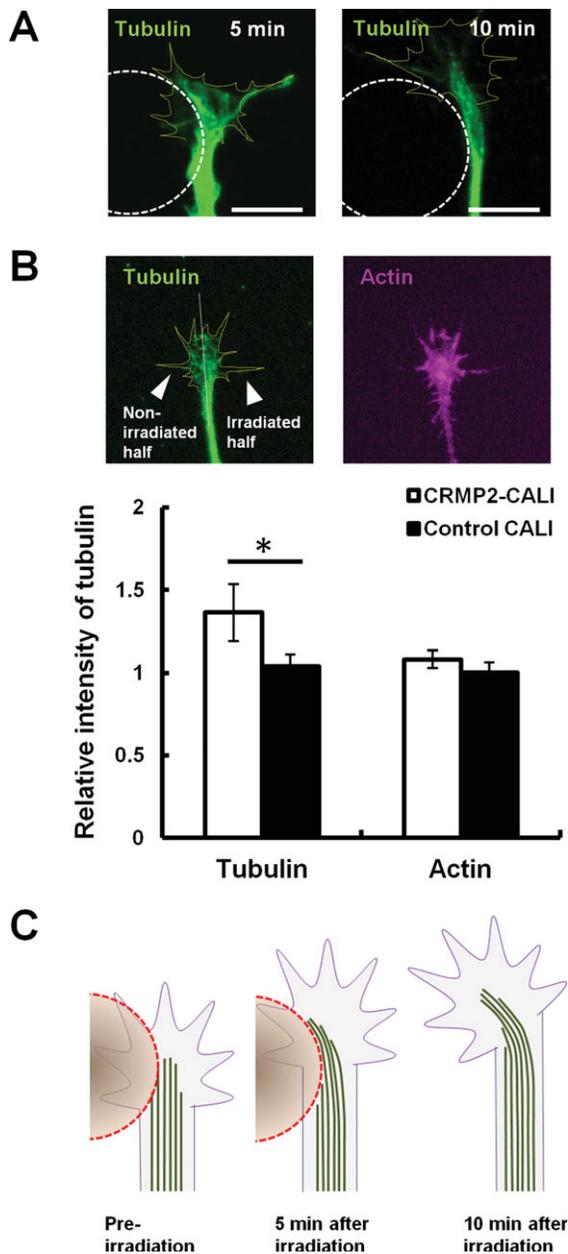

Figure 5 Localization of tubulin and actin after micro-CALI of CRMP2 in the half of the growth cone. (A) Protrusion of MTs after irradiation to the left half of the growth cone. Time indicates an interval from the start of laser irradiation. A dotted white circle indicates the laser spot. A dotted yellow line depicts growth cone perimeter. Scale bars: 10 μm. (B) Relative fluorescence intensity of tubulin and actin, defined as the average intensity in the irradiated half region of the growth cone against that in the nonirradiated half region. CRMP2-CALI ($n = 10$) and control-CALI using MG-IgG antibodies ($n = 10$) are shown. A dotted yellow line in the upper-left photograph indicates the growth cone perimeter. A solid line depicts the midline of the growth cone along the growth direction. *$p < 0.05$ by Student unpaired t-test. Error bars represent SEM. (C) A working hypothesis for the mechanism underlying turning toward the irradiated side after asymmetric application of CRMP2-CALI. A dotted red circle reveals irradiation spot. Green lines depict MTs.

of AFs both with MTs via +TIPs and with the substrate via membrane adhesion molecules in the leading edge and filopodia (Zheng et al., 1996; Challacombe et al., 1997; Nakamura et al., 2001; Buck and Zheng, 2002; Koester et al., 2007; Lowery and Van Vactor, 2009; Tojima et al., 2011). Some previous experiments regarding asymmetric disruption of these components by local pharmacological treatment demonstrated that the growth cone subsequently turned away from the treated side (Challacombe et al., 1997; Buck and Zheng, 2002; Yuan et al., 2003; Koester et al., 2007). Turning away in focal micro-CALI of CRMP1 in the growth cone would occur on the basis of this mechanism.

In contrast, focal inactivation of CRMP2 in the growth cone astonishingly forced the growth cone to turn toward the inactivated side. As micro-CALI of CRMP2 in the growth cone showed little morphological change, a bias of actin formation or membrane trafficking was less likely to induce this turning. Because focal inactivation of CRMP2 in the growth cone gave rise to protrusion of MTs toward the irradiated side of the growth cone before the onset of turning, this turning was presumably directed by alteration of MT assembly but not actin. It is reported that focal stabilization of MTs causes the growth cone to turn toward the irradiated site (Mack et al., 2000; Buck and Zheng, 2002). However, considering the data showing that micro-CALI of CRMP2 within the whole growth cone caused growth arrest of neurites, it is likely that focal inactivation of CRMP2 caused focal disassembly of MTs. Accordingly, we speculate that this turning might be caused by a mismatch of the growth rate of MTs asymmetrically across the bundle of MTs where MTs are consolidated by tightly cross-linking each other. In other words, the rate of MT elongation in the intact side would be higher than that in the CRMP2-disrupted side, causing MT bending toward the hampered side [Fig. 5(C)]. These results seem to conflict with the report that inhibition of MT polymerization by nocodazole led to turning away from the treated site (Buck and Zheng, 2002). This discrepancy was probably caused by the difference in methodology. Because the pharmacological reagents were continuously added and allowed to spread over large area including the predictive growth path of the growth cone, the growth direction of the growth cone may eventually be turned away. On the contrary, our data were obtained by an acute, spatiotemporally limited effect of CRMP2 inactivation. This phenomenon might be seen in this particular experiment. Although it is highly likely that CRMP2 exerts its function by regulating MT assembly in growth cone steering, further studies are needed to

elucidate how CRMP2 is involved in growth cone steering.

In conclusion, our present study provides the first evidence for different functions of CRMP1 and CRMP2 in neurite outgrowth and growth cone steering. This work sheds light on further understanding the concept that cooperation of a variety of molecules even among CRMP isoforms is required to attain proper growth cone navigation mechanisms.

REFERENCES

Arimura N, Inagaki N, Chihara K, Menager C, Nakamura N, Amano M, Iwamatsu A, et al. 2000. Phosphorylation of collapsin response mediator protein-2 by Rho-kinase. Evidence for two separate signaling pathways for growth cone collapse. J Biol Chem 275:23973–23980.

Arimura N, Menager C, Kawano Y, Yoshimura T, Kawabata S, Hattori A, Fukata Y, et al. 2005. Phosphorylation by Rho kinase regulates CRMP-2 activity in growth cones. Mol Cell Biol 25:9973–9984.

Buck KB, Zheng JQ. 2002. Growth cone turning induced by direct local modification of microtubule dynamics. J Neurosci 22:9358–9367.

Buel GR, Rush J, Ballif BA. 2010. Fyn promotes phosphorylation of collapsin response mediator protein 1 at tyrosine 504, a novel, isoform-specific regulatory site. J Cell Biochem 111:20–28.

Challacombe JF, Snow DM, Letourneau PC. 1997. Dynamic microtubule ends are required for growth cone turning to avoid an inhibitory guidance cue. J Neurosci 17:3085–3095.

Charrier E, Mosinger B, Meissirel C, Aguera M, Rogemond V, Reibel S, Salin P, et al. 2006. Transient alterations in granule cell proliferation, apoptosis and migration in postnatal developing cerebellum of CRMP1−/− mice. Genes Cells 11:1337–1352.

Deo RC, Schmidt EF, Elhabazi A, Togashi H, Burley SK, Strittmatter SM. 2004. Structural bases for CRMP function in plexin-dependent semaphorin3A signaling. EMBO J 23:9–22.

Fan J, Raper JA. 1995. Localized collapsing cues can steer growth cones without inducing their full collapse. Neuron 14:263–274.

Fukada M, Watakabe I, Yuasa-Kawada J, Kawachi H, Kuroiwa A, Matsuda Y, Noda M. 2000. Molecular characterization of CRMP5, a novel member of the collapsin response mediator protein family. J Biol Chem 275:37957–37965.

Fukata M, Watanabe T, Noritake J, Nakagawa M, Yamaga M, Kuroda S, Matsuura Y, et al. 2002a. Rac1 and Cdc42

capture microtubules through IQGAP1 and CLIP-170. Cell 109:873–885.

Fukata Y, Itoh TJ, Kimura T, Menager C, Nishimura T, Shiromizu T, Watanabe H, et al. 2002b. CRMP-2 binds to tubulin heterodimers to promote microtubule assembly. Nat Cell Biol 4:583–591.

Goshima Y, Nakamura F, Strittmatter P, Strittmatter SM. 1995. Collapsin-induced growth cone collapse mediated by an intracellular protein related to UNC-33. Nature 376:509–514.

Hamajima N, Matsuda K, Sakata S, Tamaki N, Sasaki M, Nonaka M. 1996. A novel gene family defined by human dihydropyrimidinase and three related proteins with differential tissue distribution. Gene 180:157–163.

Hensley K, Christov A, Kamat S, Zhang XC, Jackson KW, Snow S, Post J. 2010. Proteomic identification of binding partners for the brain metabolite lanthionine ketimine (LK) and documentation of LK effects on microglia and motoneuron cell cultures. J Neurosci 30:2979–2988.

Hu L, Papoian GA. 2010. Mechano-chemical feedbacks regulate actin mesh growth in lamellipodial protrusions. Biophys J 98:1375–1384.

Inagaki N, Chihara K, Arimura N, Menager C, Kawano Y, Matsuo N, Nishimura T, et al. 2001. CRMP-2 induces axons in cultured hippocampal neurons. Nat Neurosci 4:781–782.

Jay DG. 1988. Selective destruction of protein function by chromophore-assisted laser inactivation. Proc Natl Acad Sci USA 85:5454–5458.

Kawano Y, Yoshimura T, Tsuboi D, Kawabata S, Kaneko-Kawano T, Shirataki H, Takenawa T, et al. 2005. CRMP-2 is involved in kinesin-1-dependent transport of the Sra-1/WAVE1 complex and axon formation. Mol Cell Biol 25:9920–9935.

Kimura T, Watanabe H, Iwamatsu A, Kaibuchi K. 2005. Tubulin and CRMP-2 complex is transported via Kinesin-1. J Neurochem 93:1371–1382.

Koester MP, Muller O, Pollerberg GE. 2007. Adenomatous polyposis coli is differentially distributed in growth cones and modulates their steering. J Neurosci 27:12590–12600.

Liao JC, Roider J, Jay DG. 1994. Chromophore-assisted laser inactivation of proteins is mediated by the photogeneration of free radicals. Proc Natl Acad Sci USA 91:2659–2663.

Lowery LA, Van Vactor D. 2009. The trip of the tip: understanding the growth cone machinery. Nat Rev Mol Cell Biol 10:332–343.

Mack TG, Koester MP, Pollerberg GE. 2000. The microtubule-associated protein MAP1B is involved in local stabilization of turning growth cones. Mol Cell Neurosci 15:51–65.

Mimura F, Yamagishi S, Arimura N, Fujitani M, Kubo T, Kaibuchi K, Yamashita T. 2006. Myelin-associated glycoprotein inhibits microtubule assembly by a Rho-kinase-dependent mechanism. J Biol Chem 281:15970–15979.

Nakamura M, Zhou XZ, Lu KP. 2001. Critical role for the EB1 and APC interaction in the regulation of microtubule polymerization. Curr Biol 11:1062–1067.

Nishimura T, Fukata Y, Kato K, Yamaguchi T, Matsuura Y, Kamiguchi H, Kaibuchi K. 2003. CRMP-2 regulates polarized Numb-mediated endocytosis for axon growth. Nat Cell Biol 5:819–826.

Quach TT, Duchemin AM, Rogemond V, Aguera M, Honnorat J, Belin MF, Kolattukudy PE. 2004. Involvement of collapsin response mediator proteins in the neurite extension induced by neurotrophins in dorsal root ganglion neurons. Mol Cell Neurosci 25:433–443.

Rahajeng J, Giridharan SS, Naslavsky N, Caplan S. 2010. Collapsin response mediator protein-2 (Crmp2) regulates trafficking by linking endocytic regulatory proteins to dynein motors. J Biol Chem 285:31918–31922.

Rosslenbroich V, Dai L, Baader SL, Noegel AA, Gieselmann V, Kappler J. 2005. Collapsin response mediator protein-4 regulates F-actin bundling. Exp Cell Res 310:434–444.

Schmidt EF, Strittmatter SM. 2007. The CRMP family of proteins and their role in Sema3A signaling. Adv Exp Med Biol 600:1–11.

Su KY, Chien WL, Fu WM, Yu IS, Huang HP, Huang PH, Lin SR, et al. 2007. Mice deficient in collapsin response mediator protein-1 exhibit impaired long-term potentiation and impaired spatial learning and memory. J Neurosci 27:2513–2524.

Takei K, Chan TA, Wang FS, Deng H, Rutishauser U, Jay DG. 1999. The neural cell adhesion molecules L1 and NCAM-180 act in different steps of neurite outgrowth. J Neurosci 19:9469–9479.

Takei K, Tokushige N, Cai W, Mikoshiba K. 2000. Indirect visualization of protein loading in living DRG neurons by concomitant trituration loading of fluorescence-labeled dextran. Bioimages 8:5–9.

Tojima T, Hines JH, Henley JR, Kamiguchi H. 2011. Second messengers and membrane trafficking direct and organize growth cone steering. Nat Rev Neurosci 12:191–203.

Uchida Y, Ohshima T, Sasaki Y, Suzuki H, Yanai S, Yamashita N, Nakamura F, et al. 2005. Semaphorin3A signalling is mediated via sequential Cdk5 and GSK3beta phosphorylation of CRMP2: implication of common phosphorylating mechanism underlying axon guidance and Alzheimer's disease. Genes Cells 10:165–179.

Uchida Y, Ohshima T, Yamashita N, Ogawara M, Sasaki Y, Nakamura F, Goshima Y. 2009. Semaphorin3A signaling mediated by Fyn-dependent tyrosine phosphorylation of collapsin response mediator protein 2 at tyrosine 32. J Biol Chem 284:27393–27401.

Wang FS, Wolenski JS, Cheney RE, Mooseker MS, Jay DG. 1996. Function of myosin-V in filopodial extension of neuronal growth cones. Science 273:660–663.

Wang LH, Strittmatter SM. 1996. A family of rat CRMP genes is differentially expressed in the nervous system. J Neurosci 16:6197–6207.

Yamashita N, Mosinger B, Roy A, Miyazaki M, Ugajin K, Nakamura F, Sasaki Y, et al. 2011. CRMP5 (collapsin response mediator protein 5) regulates dendritic development and synaptic plasticity in the cerebellar Purkinje cells. J Neurosci 31:1773–1779.

Yamashita N, Uchida Y, Ohshima T, Hirai S, Nakamura F, Taniguchi M, Mikoshiba K, et al. 2006. Collapsin response mediator protein 1 mediates reelin signaling in cortical neuronal migration. J Neurosci 26:13357–13362.

Yamashita N, Morita A, Uchida Y, Nakamura F, Usui H, Ohshima T, Taniguchi M, et al. 2007. Regulation of spine development by semaphorin3A through cyclin-dependent kinase 5 phosphorylation of collapsin response mediator protein 1. J Neurosci 27:12546–12554.

Yoshimura T, Kawano Y, Arimura N, Kawabata S, Kikuchi A, Kaibuchi K. 2005. GSK-3beta regulates phosphorylation of CRMP-2 and neuronal polarity. Cell 120: 137–149.

Yuan XB, Jin M, Xu X, Song YQ, Wu CP, Poo MM, Duan S. 2003. Signalling and crosstalk of Rho GTPases in mediating axon guidance. Nat Cell Biol 5:38–45.

Yuasa-Kawada J, Suzuki R, Kano F, Ohkawara T, Murata M, Noda M. 2003. Axonal morphogenesis controlled by antagonistic roles of two CRMP subtypes in microtubule organization. Eur J Neurosci 17:2329–2343.

Zheng JQ, Wan JJ, Poo MM. 1996. Essential role of filopodia in chemotropic turning of nerve growth cone induced by a glutamate gradient. J Neurosci 16:1140–1149.

Zhou FQ, Cohan CS. 2004. How actin filaments and microtubules steer growth cones to their targets. J Neurobiol 58:84–91.